



# Theoretical study on vapour phase Beckmann rearrangement of cyclohexanone oxime over a high silica MFI zeolite

Masaya Ishida<sup>a</sup>, Tatsuya Suzuki<sup>b</sup>, Hiroshi Ichihashi<sup>b</sup>, Akinobu Shiga<sup>a,\*</sup>

<sup>a</sup> Tsukuba Research Laboratory, Sumitomo Chemical Co., Ltd., Kitahara 6, Tsukuba, Ibaraki 300-3294, Japan

<sup>b</sup> Basic Chemicals Research Laboratory, Sumitomo Chemical Co., Ltd., Sobiraki, Niihama 792-5821, Japan

## Abstract

We have studied an activation mechanism of cyclohexanone oxime in a cavity of high silica MFI zeolite by using PIO analysis proposed by Fujimoto et al. DFT calculation reveals that the bond length of N–OH becomes longer when water coordinates on oxygen of oxime. The PIO clearly shows out-of-phase interaction between N and O. This out-of-phase interaction is also observed in the PIO of oxime/MFI zeolite cluster model and weakens the N–O bond. Hydrogen bond of Si–OH of nest silanols to oxime is a trigger of vapour phase Beckmann rearrangement.

© 2003 Elsevier B.V. All rights reserved.

**Keywords:** Cyclohexanone; Beckmann rearrangement; Double numerical polarization

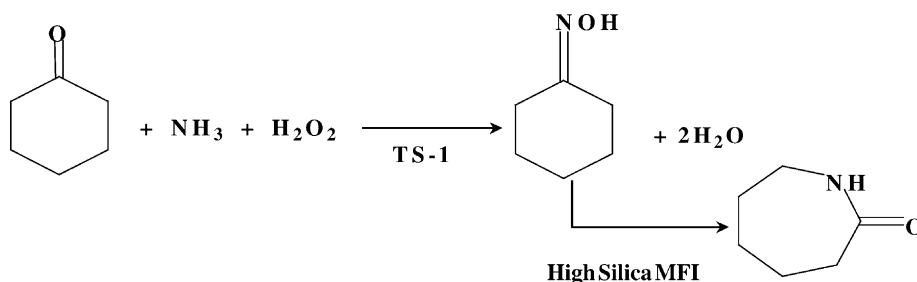
## 1. Introduction

A catalyst mainly composed of high silica MFI zeolite (silicalite-1) has been developed for the vapour phase Beckmann rearrangement of cyclohexanone oxime to  $\epsilon$ -caprolactam. This catalyst does not possess acidity that can be detected by ammonia TPD. Sumitomo Chemical Co., Ltd., has begun to manufacture caprolactam with a new vapour phase process by applying this catalyst in 2003 spring [1]. The process consists of two catalytic processes. The first stage is the ammoximation developed by EniChem SpA in Italy, and the second is the vapor phase Beckmann rearrangement developed by Sumitomo Chemical Co., Ltd., in Japan. Caprolactam is manufactured from cyclohexanone, ammonia and hydrogen peroxide via cyclohexanone oxime with the aid of two catalysts.

Caprolactam is obtained in good yield without producing ammonium sulfate as a by-product. As the only by-product of the process is water as shown in the Scheme 1, the process is so called “green process”.

Sato et al. reported the relationship between the catalytic activities and Si/Al atomic ratio. As increasing the ratio the activity and selectivity increased. The zeolites having the ratio higher than 1000, give high selectivity to  $\epsilon$ -caprolactam with high conversion [2]. They also reported that the acidity and selectivity were drastically improved by the treating the high silica zeolites with chlorotrimethylsilane vapor [3]. Kitamura et al. reported the same improvement was attained by methanol instead of the silane [4]. Astonishingly, the life of the catalyst is improved by addition of ammonia in the reaction system without affecting the conversion and the selectivity [5]. The reaction mechanism of Beckmann rearrangement under the vapour phase conditions can be considered the same as in the liquid phase, namely the alkyl group in anti-position against

\* Corresponding author. Tel.: +81-298-64-4160;  
fax: +81-298-64-4729.  
E-mail address: [aas55@mail2.accsnet.ne.jp](mailto:aas55@mail2.accsnet.ne.jp) (A. Shiga).



Scheme 1. Combined process: ammoximation and vapour phase Beckmann rearrangement.

the hydroxyl group of the oxime migrates to the N atom position [6].

Nest silanols located just inside of the pore mouth of the MFI zeolite are supposed to be the active site of the catalyst. We propose that the N–OH group of cyclohexanone oxime molecule adsorbed on the zeolite surface is coordinated by OH groups of the nest silanols with hydrogen bonding, and the coordination seems to play an important role for the reaction. The importance of nest silanols and the mechanism under the vapour phase conditions have been also reported [6,7].

In this paper, we present an activation mechanism of cyclohexanone oxime in a pore of high silica MFI zeolite by using PIO analysis proposed by Fujimoto et al. [8].

## 2. Calculation method

### 2.1. DFT calculation

Here, as our simplified models of hydrogen bonding system, we supposed  $\text{C}_6\text{H}_{10}\text{N–OH}$ /water systems with one or two water molecules which may correspond to the –OH groups of nest silanol. At first, we have investigated the influence of hydrogen bonding for cyclohexanone oxime using the models in order to look at how cyclohexanone oxime is activated in the initial process of Beckmann rearrangement. In our models, one or two water molecules were coordinated to N or O atoms of N–OH group of cyclohexanone oxime, respectively. Then, we have performed geometry optimization by DFT calculation for these models and have looked at the change of N–O bond length. All DFT calculations were carried out with GGA-PW91 functionals and double numerical polarization (DNP) basis sets of DMol<sup>3</sup> quantum mechanical program, and

Molecular modelings were also executed by Materials Studio 2.1 [9].

### 2.2. PIO analysis

Next, followed by DFT calculation, we have executed PIO analysis for our optimized models in order to clarify the activation mechanism of cyclohexanone oxime by hydrogen bonding from a point of view of orbital interactions. Moreover, we have executed the same analysis for cluster models consisted of cyclohexanone oxime and a part of MFI zeolite with nest silanols. Our nest silanol model was obtained from another cluster of MFI straight channel optimized using DMol<sup>3</sup>. All dangling bonds were terminated with hydrogen atom.

PIO analysis, proposed by Fujimoto et al, is a method for unequivocally determining the orbitals which should play dominant roles in chemical interactions between two systems, [A] and [B]. In this study, [A] is oxime and [B] is water or silanol. The location of the oxime in the cavity of the zeolite is assumed. The MOs of [A], [B] and the combined system [C] were calculated by the extended Hückel method. The extended Hückel parameters are given in the Appendix A. PIOs were obtained by applying the procedure that was proposed by Fujimoto et al. It is summarized as follows:

- (1) We expand the MOs of a complex in terms of the MOs of two fragment species, to determine the expansion coefficients  $c_{i,f}$ ,  $c_{m+j,f}$  and  $d_{k,f}$ ,  $d_{n+l,f}$  in Eq. (1)

$$\Phi_f = \sum_{i=1}^m c_{i,f} \phi_i + \sum_{j=1}^{M-m} c_{m+j,f} \phi_{m+j} + \sum_{k=1}^n d_{k,f} \psi_k + \sum_{l=1}^{N-n} d_{n+l,f} \psi_{n+l}, \quad f = 1, 2, \dots, m+n, \quad (1)$$

where  $\Phi$ , is a MO of the complex [C],  $\phi$  and  $\psi$  are the MOs of the fragment [A] and fragment [B], respectively,  $m$  and  $n$  indicate the number of the occupied MOs of A and of B, respectively, and  $M$  and  $N$  represent the number of the MOs of A and of B, respectively,

- (2) we construct an interaction matrix, which represents the interaction between the MOs of the fragment [A] and the MOs of the fragment [B]

$$P = \begin{pmatrix} p_{i,k} & p_{i,n+l} \\ p_{m+j,k} & p_{m+j,n+l} \end{pmatrix} \quad (2)$$

in which

$$p_{i,k} = n_{t,u} \sum_{f=1}^{m+n} c_{i,f} d_{k,f}, \quad i = 1 \sim m, \quad k = 1 \sim n$$

$$p_{i,n+l} = n_{t,u} \sum_{f=1}^{m+n} c_{i,f} d_{n+l,f}, \quad i = 1 \sim m, \quad l = 1 \sim N - n$$

$$p_{m+j,k} = n_{t,u} \sum_{f=1}^{m+n} c_{m+j,f} d_{k,f}, \quad j = 1 \sim M - m, \quad k = 1 \sim n$$

$$p_{m+j,n+l} = n_{t,u} \sum_{f=1}^{m+n} c_{m+j,f} d_{n+l,f}, \quad j = 1 \sim M - m, \quad l = 1 \sim N - n$$

- (3) we get transformation matrix,  $U^A$  (for A) and  $U^B$  (for B) by

$$\tilde{P} P U^A = U^A \Gamma \quad (3)$$

$$U_{s,v}^B = (\gamma_v)^{-1/2} \sum_r^N p_{r,s} U_{r,v}^A \quad v = 1, 2, \dots, N \quad (4)$$

- (4) finally we obtain the PIOs by Eqs. (5) and (6)

$$\phi'_v = \sum_r^N U_{r,v\phi r}^A \quad (\text{for A}) \quad (5)$$

$$\psi'_v = \sum_s^N U_{s,v\psi s}^B \quad (\text{for B}) \quad (6)$$

The  $N \times M$  ( $N \leq M$ ) orbital interactions in the complex C can thus be reduced to the interactions of  $N$  PIOs,  $N$  indicating the smaller of the numbers of MOs of the two fragments, A and B. All calculations were carried out on LUMMOX<sup>TM</sup> system [10].

### 3. Results and discussion

#### 3.1. The influence of water coordination on cyclohexanone oxime

The bird's views of optimized structures of  $C_6H_{10}N-OH$ /water systems obtained by DFT calculation are shown in Fig. 1. The calculated bond length of N–OH is 1.428 Å, but it becomes longer when a water molecule coordinates on oxygen atom of oxime group (Fig. 1c). Coordination of two water molecules makes the bond length more elongated (Fig. 1d). On the other hand, the bond length does not change in case that one water molecule coordinates on nitrogen

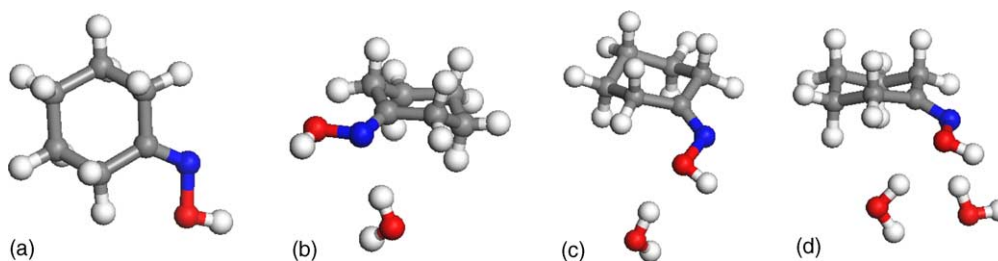


Fig. 1. DFT calculation results; bird's views of optimized structures of  $C_6H_{10}NOH$ /water systems and their N–O bond length: R(Å). Most dark circles of (a)–(d) represent Nitrogen atom of oxime group. OH group is linked to N atom directly. (a): oxime R(N–OH) = 1.428 (b): one water molecule hydrogen bonded to N atom of oxime R(N–OH) = 1.429 (c): one water molecule hydrogen bonded to O atom of oxime R(N–OH) = 1.440 (d): two water molecules hydrogen bonded to O atom of oxime R(N–OH) = 1.460.

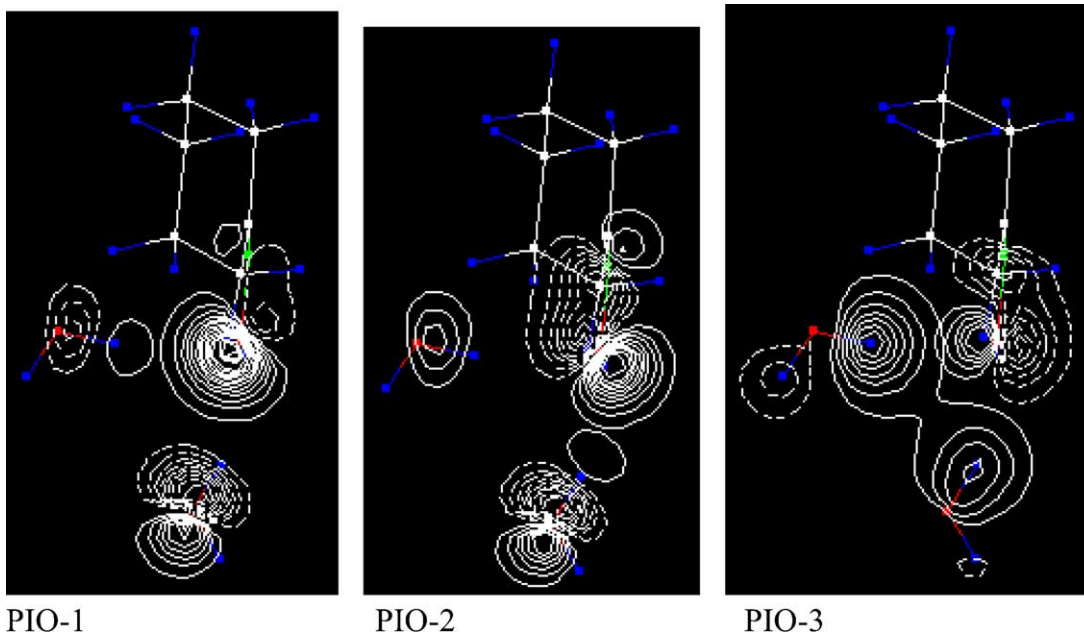


Fig. 2. Contour maps of PIO-1, PIO-2 and PIO-3 of  $C_6H_{10}N-OH/(H_2O)_2$  system. Cartesian coordinates of the optimized geometry in Fig. 1d were used. White solid lines stand for a cyclohexanone ring and two water molecules is set to left and bottom side in figures. Oxime group is located between cyclohexanone ring and a water molecule at bottom side. PIO-1 shows in-phase interaction of hydrogen bonding between oxime group and a water at left side. PIO-2 shows mainly out-of-phase interaction of N–O bond. PIO-3 also shows in-phase interaction of hydrogen bonding as same as PIO-1.

atom (Fig. 1b). These results clearly show that hydrogen bonding to oxygen atom of oxime group makes N–OH chemical bond weakened. Thus, we believe that hydrogen bonding plays an important role to activate cyclohexanone oxime in the initial process of Beckmann rearrangement.

### 3.2. PIO analysis of the two waters coordinated cyclohexanone oxime

We have done PIO analysis of the two waters hydrogen bonded state: Fig. 1d. Eigen values of PIO (not shown in here) tell us that almost all of the interactions

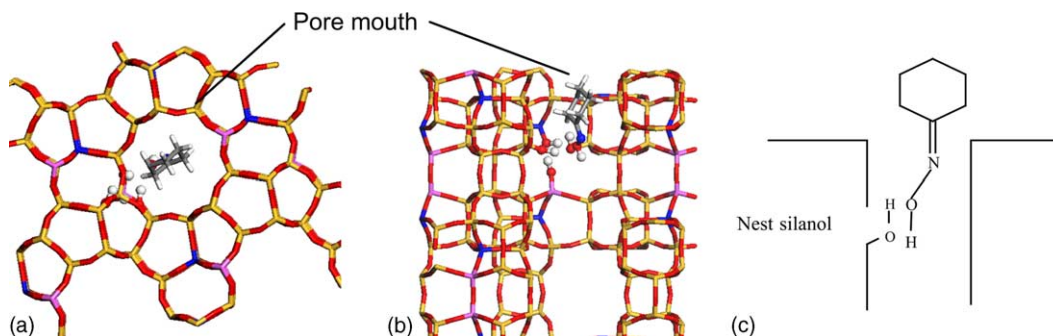


Fig. 3. A model of coordination of cyclohexanone oxime on the active site (a) front section of a straight channel, (b) side section of the channel (a), (c) an image to help understanding the view of (b).

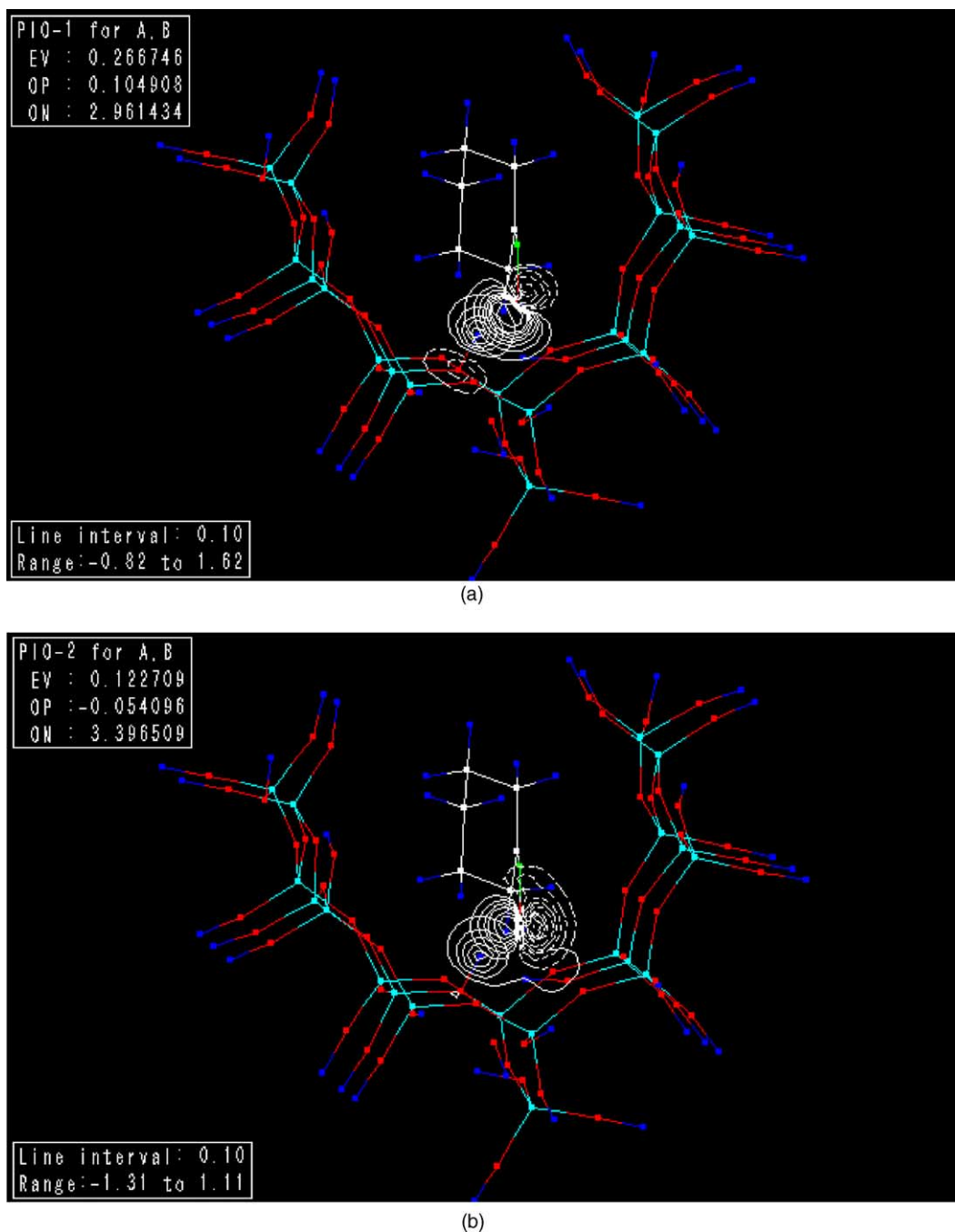
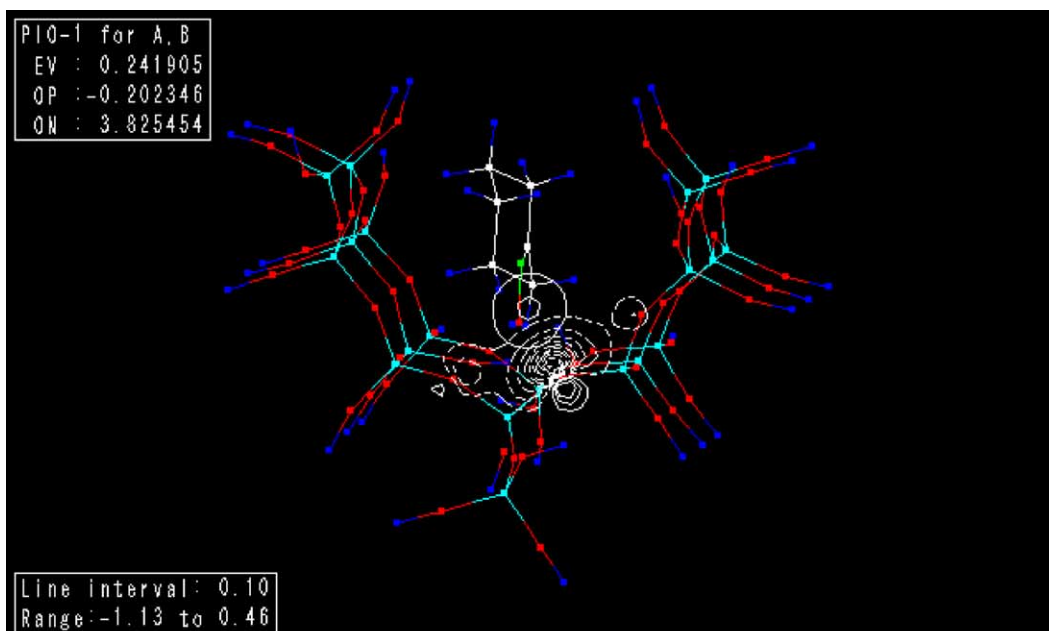
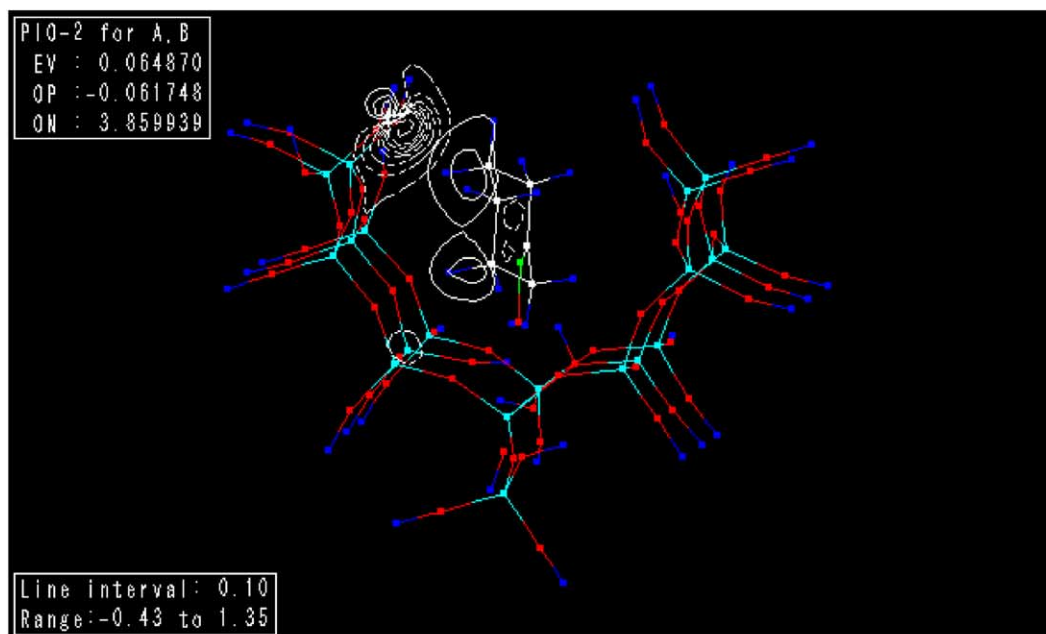


Fig. 4. Contour maps of (a) PIO-1 and (b) PIO-2 of model 1 (syn-form):  $\text{Si}_{19}\text{O}_{55}\text{H}_{34}\text{-syn-C}_6\text{H}_{10}\text{NOH}$ . The structure of nest silanols is shown in the bottom of the figures and one silanol group is directed to the inside of zeolite channel. N–OH group of oxime interacts with it. PIO-1 (a) shows in-phase interaction between oxygen atom of N–OH group and Hydrogen atom of the silanol group. PIO-2 shows same interaction as same as PIO-1 and out-of-phase interaction between Nitrogen atom and Oxygen atom of the oxime.



(a)



(b)

Fig. 5. Contour maps of (a); PIO-1 and (b); PIO-2 of model 2 (anti-form):  $\text{Si}_{19}\text{O}_{55}\text{H}_{34}$ -anti- $\text{C}_6\text{H}_{10}\text{NOH}$ . Cyclohexanone oxime is coordinated with the sixth ring to the nest silanols. PIO-1 shows out-of-phase interaction between cyclohexanone ring and silanols. PIO-2 also shows unrelated interaction to silanols.



are represented in only three PIOs, PIO-1, PIO-2 and PIO-3. The largest one is PIO-1 and the second one is PIO-2. Contour maps of PIO-1, PIO-2 and PIO-3 of the state are shown in Fig. 2.

PIO-1, PIO-2 and PIO-3 express in-phase interaction between the oxygen of oxime and the hydrogen of waters, these are the origin of the hydrogen bond, while these PIOs also show out-of-phase interaction between the oxime nitrogen and the oxime oxygen, especially clearly in PIO-2. These out-of-phase interactions weaken the N–O bond.

### 3.3. PIO analysis of cyclohexanone oxime in the cavity of MFI zeolite

We cut off  $\text{Si}_{19}\text{O}_{55}\text{H}_{34}$  cluster from the cavity of the 10 membered ring straight channel of MFI zeolite. Cyclohexanone oxime is put into the cavity from the direction of N–O bond keeping the axis of N–O bond parallel with the center line of the cavity. This one is a syn-form and the reverse one, which is put oxime into the cavity from the direction of cyclohexane ring, is an anti-form. A schematic illustration of oxime coordinated to nest silanols in the cavity of MFI zeolite are shown in Fig. 3.

The results of PIO analysis are summarized in Table 1.

The total energy of the syn-form is almost same as that of the anti-form, however the interactions between the  $\text{Si}_{19}$  cluster and the oxime are quite different from each other. Overlap population of PIO-1(0.1049) shows attractive interaction in the case of syn-form, whereas in the case of anti-form, overlap population of PIO-1(−0.2023) shows repulsive interaction. As shown Fig. 4, clear in phase interactions are observed in the case of the syn-form because of hydrogen bond between the  $\text{Si}_{19}$  cluster and the oxime.

In Fig. 4, especially in PIO-2, we can also see out-of-phase interaction between the oxime nitrogen

and the oxime oxygen, as observed in the case of oxime/waters system.

This out-of-phase interaction weakens the N–O bond of the oxime. On the other hand, in the case of anti-form, as shown Fig. 5, main interactions are repulsion between the cyclohexane ring and the wall of the zeolite. In addition to this, we can not observe any evidence of the hydrogen bond in Fig. 5. Therefore, we can conclude that the N–O bond activation is difficult in the anti-form.

## 4. Conclusion

DFT calculation reveals that the bond length of N–OH becomes longer when water coordinates on oxygen of oxime. The PIO analysis proposed by Fujimoto et al., clearly shows out-of-phase interaction between N and O. This out-of-phase interaction is also observed in the PIO of oxime/MFI zeolite cluster models and weakens the N–O bond. Hydrogen bond of Si–OH of nest silanols to oxime is a trigger of vapour phase Beckmann rearrangement.

## Acknowledgements

We thank Professor H. Fujimoto for helpful advice and Sumitomo Chemical Co. Ltd., for permission to publish.

## Appendix A

Coulomb integrals and orbital exponents are listed in Table A.1.

Table A.1  
Extended Hückel parameters

Orbital	H <sub>ii</sub> (eV)	$\zeta$ 1
H1s	−13.60	1.30
C2s	−21.40	1.625
C2p	−11.40	1.625
N2s	−26.00	1.950
N2p	−13.40	1.950
O2s	−32.30	2.275
O2p	−14.80	2.275
Si3s	−17.30	1.383
Si3p	−9.20	1.383
Si3d	−6.00	1.383

Table 1

Total energy and overlap population of PIO-1 and PIO-2 of model 1 (syn-form):  $\text{Si}_{19}\text{O}_{55}\text{H}_{34}$ -syn- $\text{C}_6\text{H}_{10}\text{NOH}$  and model 2 (anti-form):  $\text{Si}_{19}\text{O}_{55}\text{H}_{34}$ -anti- $\text{C}_6\text{H}_{10}\text{NOH}$

	Model 1 (syn-form)	Model 2 (anti-form)
Total energy (eV)	−9751.18	−9751.48
Overlap population of PIO-1	0.1049	−0.2023
Overlap population of PIO-2	−0.0541	−0.0617

## References

- [1] H. Ichihashi, M. Kitamura, *Catal. Today* 73 (2002) 23.
- [2] H. Sato, K. Hirose, S. Nakamura, in: *Proceedings of the Seventh IZC*, 1986, p. 755.
- [3] H. Sato, K. Hirose, M. Kitamura, Y. Nakamura, *Shokubai* 31 (1989) 136.
- [4] M. Kitamura, H. Ichihashi, *Stud. Sci. Catal.* 90 (1994) 67.
- [5] H. Ichihashi, M. Kitamura, H. Kajikuri, E. Tasaka, *USP* 5,354,859 (1992).
- [6] H. Kajikuri, M. Kitamura, H. Ichihashi, in: *Proceedings of the KISPOC-VII*, Fukuoka, Japan, 1997, p. 507.
- [7] G.P. Heitmann, G. Dahlhoff, W.F. Hoelderrich, *J. Catal.* 186 (1999) 12.
- [8] H. Fujimoto, T. Yamasaki, N. Koga, *J. Am. Chem. Soc.* 107 (1985) 6157.
- [9] DMol<sup>3</sup> Quantum Mechanical Program and Materials Studio 2.1 Molecular Modeling System, Accelrys Inc., San Diego, CA, All graphics of Figs. 2 and 4 were obtained with using Materials Studio 2.1.
- [10] H. Katsumi, Y. Kikuzono, M. Yoshida, A. Shiga, H. Fujimoto, Least Unified Meta-Molecular Orbital Calculation System (LUMMOX<sup>TM</sup>), Sumitomo Chemical Co., Ltd., Tokyo, 1999.